IX International Conference on Particle-Based Methods
PARTICLES 2025
J. Bonet, M. Cremonesi, A. Franci, A. Gil (Eds)

NUMERICAL CALCULATION MODEL FOR MR FLUID BEHAVIOR IN MAGNETIC FIELD - PARTICLES 2025

SOTA TSUJIMOTO[*1], TOWA KIKUGAWA[1], KATSUHIRO HIRATA[1], FUMIKAZU MIYASAKA[1], SHINOBU KAMADA[2], YUKIHIRO HANAJIMA[2], SHO TANIGUCHI[2], PRIYO BAYU RAMADHAN[2] AND NOBUHIRO KAITO[3]

[1] The University of Osaka
Suita Campus, Osaka 565-0871, Japan
e-mail: info@osaka-u.ac.jp, web page: https://www.osaka-u.ac.jp/en

[2] THK CO., LTD.
Techno Center, Tokyo 144-0033, Japan
e-mail: s.kamada@thk.co.jp, y.hanajima@thk.co.jp, sh.taniguchi@thk.co.jp, p.ramadhan@thk.co.jp
web page: https://www.thk.com/

[3] COSMO OIL LUBRICANTS CO., LTD.
Technical Dept, Tokyo 104-8352, Japan
e-mail: nobuhiro_kaito@cosmo-oil.co.jp, web page: https://www.cosmo-lube.co.jp/eng/

Key words: DEM, MPS, MR fluid, Magnetic Field.

Abstract. Recently, Magnetorheological (MR) fluids have been attracting attention as a type of functional fluid. MR fluids have the property that the ferromagnetic particles form chain-like clusters and change their viscosity significantly in response to the applied magnetic field strength. MR fluids are expected to be applied to vibration control systems such as dampers, clutches, brakes and so on because of their ability to change viscosity electrically, reversibly, and continuously on the order of milliseconds. However, the mechanism is complex, and experimental approaches are the most common, requiring a large number of experiments on actual equipment.
Therefore, it is expected to analyze the behavior of magnetic particles inside the fluids by numerical simulation and clarify their dynamic characteristics for determining the optimal parameters for application to actual equipment. In this study, we propose a numerical analysis method that couples the particle method and the magnetic moment method, focusing on the change in shear stress due to the magnetic field in MR fluids. Also, we evaluate the effects of magnetic particle density and external magnetic field strength on the cluster formation speed and particle behavior.

1 INTRODUCTION

Magnetorheological (MR) fluid is a solid-liquid mixture in which ferromagnetic particles about several tens of micrometers in size are uniformly dispersed mainly in a hydrocarbon-based oil medium. When an external magnetic field is applied, these particles form chain-like

clusters. As a result, the viscosity of the fluid changes significantly depending on the magnetic field strength. The viscosity can also be controlled reversibly and continuously within milliseconds by electrical input. Because of this unique property, MR fluids are expected to a wide range of applications in mechanical control systems [1]. In particular, MR fluid-based automotive dampers have attracted attention as effective gears for improving performance. Unlike conventional hydraulic systems, they enable semi-active control in response to external disturbances [2]. However, the characteristics of MR fluids have so far been mainly evaluated through experiments. Thus, the practical implementation of MR fluid-based dampers requires repeated prototyping and testing to determine optimal control parameters. An additional issue is the high particle concentration in MR fluids, which makes it difficult to observe their three-dimensional particle distribution using microscopy. Therefore, numerical simulations are considered a promising approach for clarifying the behavior of ferromagnetic particles inside MR fluids [3]-[5].

In this study, the particle method is employed to represent the behavior of magnetic particles in MR fluids, since it can directly represent the shape and distribution of individual particles. The particle method does not require a mesh and allows the direct treatment of free surfaces. Therefore, it is considered effective for analyzing the behavior of MR fluids subjected to large deformations. Furthermore, by coupling it with the magnetic moment method, which is a technique for mesh free magnetic field analysis, the motion of magnetic particles in MR fluids is calculated.

2 ANALYSIS METHOD

Since MR fluids are composed of magnetic particles dispersed in a solvent, they must be treated as a coupled problem between the fluid and particle behaviors. In this analysis, Discrete Element Method (DEM) [6] is applied for particle analysis, and the hydrodynamic drag force is calculated using the Basset-Boussinesq-Oseen (BBO) equation [7]. Furthermore, the magnetic moment method [8],[9] is employed to compute magnetic interactive force between particles. This method is highly compatible with the particle method. In the following, each analysis method and their coupling method are described.

2.1 Particle analysis

DEM is applied to compute the collision and rotational motion of magnetic particles. DEM is a method of calculating powder behavior by approximating individual powder particles as particles and calculating their collisions. In the case of two particles, the normal component $\boldsymbol{f}_{\mathrm{n}}$ and tangential component $\boldsymbol{f}_{\mathrm{s}}$ of the force acting between the particles are expressed by Eq. (1), (2), and (3). where $\boldsymbol{u}_{\mathrm{n}}$ is the normal displacement, $\boldsymbol{v}_{\mathrm{n}}$ is the normal velocity, $\boldsymbol{u}_{\mathrm{s}}$ is the tangential displacement, $\boldsymbol{v}_{\mathrm{s}}$ is the tangential velocity, k_{n} is the normal spring constant, c_{n} is the normal viscous damping coefficient, k_{s} is the tangential spring constant, and c_{s} is the tangential viscous damping coefficient. When sliding is considered, the tangential force is modified using the friction coefficient μ.

$$\boldsymbol{f}_{\mathrm{n}} = -k_{\mathrm{n}}\boldsymbol{u}_{\mathrm{n}} - c_{\mathrm{n}}\boldsymbol{v}_{\mathrm{n}} \tag{1}$$

$$\boldsymbol{f}_{\mathrm{s}} = -k_{\mathrm{s}}\boldsymbol{u}_{\mathrm{s}} - c_{\mathrm{s}}\boldsymbol{v}_{\mathrm{s}} \tag{2}$$

$$\boldsymbol{f'}_{\mathrm{s}} = \begin{cases} \dfrac{\boldsymbol{f}_{\mathrm{s}}}{|\boldsymbol{f}_{\mathrm{s}}|}\mu|\boldsymbol{f}_{\mathrm{n}}| & (|\boldsymbol{f}_{\mathrm{s}}| > \mu|\boldsymbol{f}_{\mathrm{n}}|) \\ \boldsymbol{f}_{\mathrm{s}} & Otherwise \end{cases} \tag{3}$$

From the above, the translational force $\boldsymbol{F_c}$ and the rotational moment $\boldsymbol{T_c}$ due to the contact forces between particles are expressed by Eq. (4), (5). where r is the particle radius.

$$\boldsymbol{F_c} = \boldsymbol{f'}_{\mathrm{s}} + \boldsymbol{f}_{\mathrm{n}} \tag{4}$$

$$\boldsymbol{T_c} = r\boldsymbol{n_{ij}} \times \boldsymbol{f'}_{\mathrm{s}} \tag{5}$$

2.2 Fluid analysis

In the fluid analysis, the BBO equation (Eq. (6)) is used to compute the interaction between particles and fluid. This equation is applicable to particles moving unsteadily in low-Reynolds-number flows. It is based on the analytical solution of the Navier–Stokes equations for unsteady Stokes flow. The first term represents the instantaneous resistance due to fluid viscosity, known as Stokes drag. The second term corresponds to the added mass resulting from the inertia of the surrounding fluid. The third term represents the history force arising from unsteady viscous effects. In this analysis, the third term is neglected because its influence is considered to be negligible. where ρ is the fluid density, γ is the kinematic viscosity, μ is the fluid viscosity coefficient, and C_D is the drag coefficient. The drag coefficient depends on the Reynolds number, and using DEM, it is generally expressed by Eq. (7). Furthermore, for spherical particles, the Reynolds number is given by Eq. (8).

$$\boldsymbol{F_l} = -\frac{1}{2}\pi C_D r^2 \rho \boldsymbol{v}^2 - \frac{2}{3}\pi\rho r^3 \dot{\boldsymbol{v}} - 6\pi\mu r^2 \int_{-\infty}^{t} \frac{\dot{\boldsymbol{v}}}{\sqrt{\pi\gamma(t-\tau)}} d\tau \tag{6}$$

$$C_D = \begin{cases} \dfrac{24}{Re}(1 + 0.15Re^{0.687}) & (Re < 1000) \\ 0.44 & Otherwise \end{cases} \tag{7}$$

$$Re = \frac{2\boldsymbol{v}\rho r}{\mu} \tag{8}$$

2.3 Magnetic field analysis

In the magnetic field analysis, the magnetic moment method is employed. This method is highly compatible with DEM because both methods employ meshfree method. It calculates the magnetization at any position based on the positions of magnetized particles or sources.

Consider a source with magnetization $\boldsymbol{M}$ in space, and at an arbitrary point P at a distance r from it. In this case, when the magnetization $\boldsymbol{M}$ is constant in a closed domain $\boldsymbol{V}$, the magnetic field intensity $\boldsymbol{H_c}$ at point P due to the magnetization $\boldsymbol{M}$ can be calculated as follows. (Eq. (9)) where μ_0 is the permeability in free space.

$$\boldsymbol{H_C} = -\frac{1}{4\pi\mu_0}\nabla\left\{\int_V \boldsymbol{M}\cdot\nabla\left(\frac{1}{r}\right)dV\right\} \tag{9}$$

Also, the magnetization of each magnetic particle element can be calculated by superposing the magnetizations of all magnetic particle elements and the magnetic field produced by the sources. However, the magnetic field from each element cannot be determined explicitly, since the magnetization induced within magnetic particles interacts with each other. Therefore, the magnetization of each magnetic particle element is considered as the result of the contributions from all other elements. In this approach, the following governing equations are solved simultaneously for all magnetized particle elements. where $\boldsymbol{M}_{i,j}$ is the magnetization of particle elements i, j, χ_i is the magnetic susceptibility, n is the number of magnetic particle elements, $\boldsymbol{H}_i$ is the magnetic field intensity at the position of particle element i, and $\boldsymbol{r}_{ij}$ is the distance vector.

$$\boldsymbol{M}_i + \frac{\chi_i}{4\pi}\sum_j^n \nabla\left\{\int_V \boldsymbol{M}_j\cdot\nabla\left(\frac{1}{\boldsymbol{r}_{ij}}\right)dV\right\} = \chi_i\mu_0\boldsymbol{H}_i \tag{10}$$

From the above, the magnetization $\boldsymbol{M}$ at each particle position and the magnetic field intensity $\boldsymbol{H}$ at the same location are obtained. Using these values, the magnetic force per unit volume $\boldsymbol{F_m}$ acting on a single magnetic particle is calculated. (Eq. (11))

$$\boldsymbol{F_m} = \boldsymbol{M}\cdot\nabla\boldsymbol{H} \tag{11}$$

2.4 Coupling methods

In this section, the coupled algorithm of the analysis methods, as described in the previous sections, is presented. The flowchart of the analysis is shown in Fig. 1. First, the contact forces between particles are calculated using DEM for the magnetic particles within the analysis domain. Next, the fluid forces acting on each particle are computed using the velocity and acceleration components obtained in the previous step. Then, the magnetic particles are treated as magnetic elements in the magnetic moment method, and the magnetization at each particle position is calculated to determine the magnetic forces. This approach eliminates the need to divide the magnetic particles into elements, as is done in the finite element method. Each particle can serve directly as an element, which also avoids the need for model conversion between analyses.

Finally, the contact force $\boldsymbol{F_c}$, the fluid force $\boldsymbol{F_l}$, and the magnetic force $\boldsymbol{F_m}$ are applied as external forces in the equations of motion, updating the positions of all particles. (Eq.(12)) For this analysis, other forces, such as gravity and intermolecular forces, are neglected. where m is the particle mass, and $\boldsymbol{p}$ is the particle position vector.

$$m\frac{d}{dt^2}\boldsymbol{p} = \boldsymbol{F_c} + \boldsymbol{F_l} + \boldsymbol{F_m} \tag{12}$$

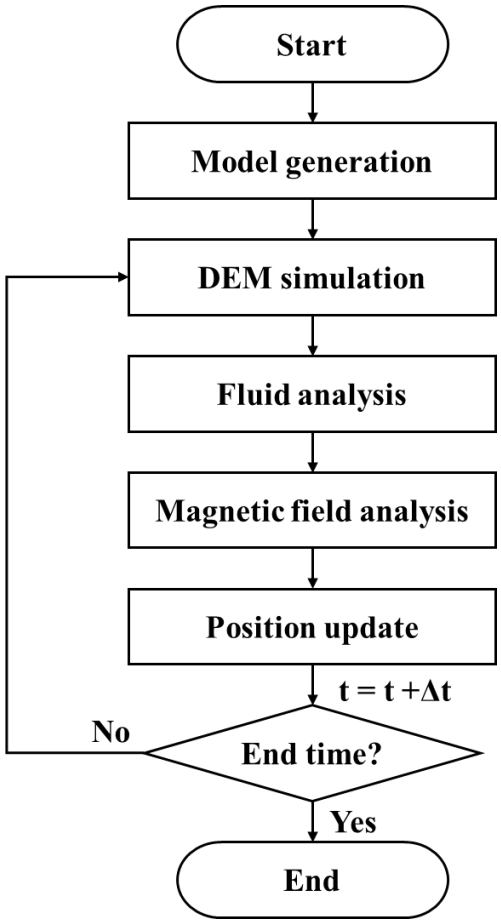

Fig. 1 Flowchart of the analysis.

3 NUMERICAL CALCULATIONS

3.1 Analysis model and conditions

The behavior of MR fluid under a magnetic field was calculated using the methods described above. The analysis model of this study is shown in Fig. 2. The coordinate axes were defined as illustrated, and the computational domain was a cube with a side length of 0.1 mm. Upper and lower magnetic walls were placed perpendicular to the z-axis. Periodic boundary conditions were applied in the x- and y-directions. Spherical magnetic particles were randomly distributed in the domain to achieve a concentration of about 70 wt%. The magnetic particles were assumed to be the carbonyl iron with the diameter of 10 μm, the density of 7870 kg/m³, and the relative permeability of 3000. The dispersion medium was the mineral oil with the density of 828.5 kg/m³ and the viscosity coefficient of 0.01. The permanent magnets magnetized along the z-axis (0.2 mm × 0.2 mm × 0.1 mm) were placed above and below the computational domain. The magnetic field was established in the domain at the start of the analysis. The magnetization $\boldsymbol{M}$ of the magnets was set to 0.1 T, 0.3 T, and 0.5 T in separate cases. Other analysis conditions are summarized in Table 1.

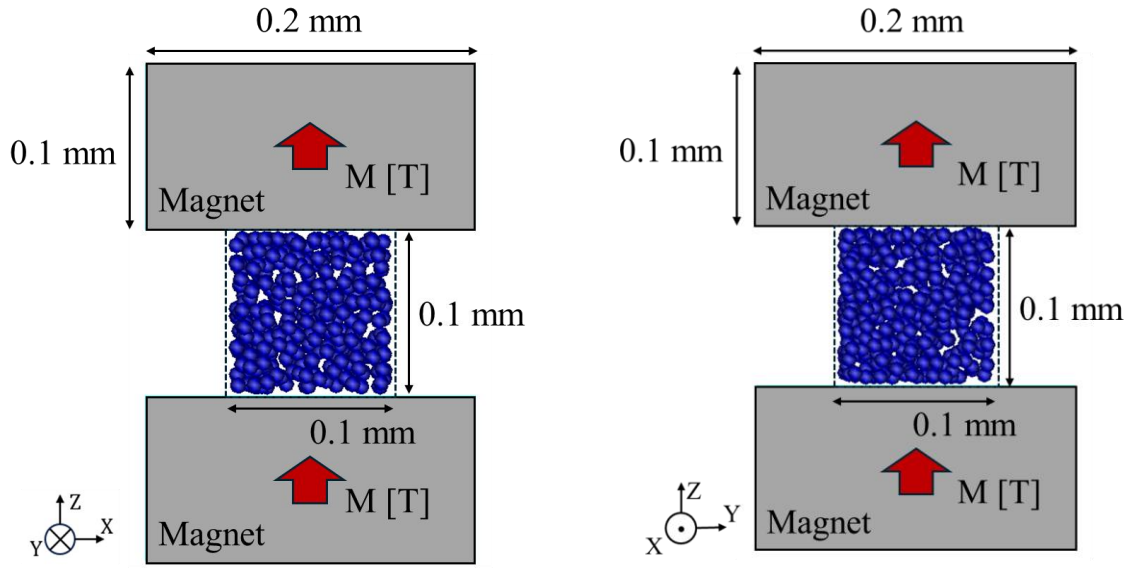

(a) View from -y-direction. (b) View from +x-direction.

Fig. 2 Analysis model.

Table 1 Analysis conditions.

Number of particles	362
Particle diameter [mm]	0.01
Density of powder [kg/m^3]	7870
Relative permeability of magnetic particles	3000
Density of fluid [kg/m^3]	828.5
Viscosity coefficient of fluid [Pa・s]	0.01
Spring constant [N/m]	3.0
Viscous damping coefficient [N・s/m]	1.0×10^{-6}
Friction coefficient	0.5
Time interval [s]	1.0×10^{-7}

3.2 Magnetic particles behavior in stationary fluid

As a result of the analysis, the time variation of MR fluid behavior under the magnetization of 0.3 T in the permanent magnets is shown in Fig. 3. It was confirmed that magnetic particles in the fluid formed clusters over time. At the initiation of the analysis, the magnetic particles were uniformly dispersed throughout the fluid, but they subsequently underwent aggregation. At 5 ms, several chain-like clusters aligned along the z-axis were formed. These clusters acted as sources of magnetomotive force generated by the permanent magnets placed above and below, and they are considered to have formed along the flux lines of the applied magnetic field.

Subsequently, the time variation of the number of clusters under different magnetization strengths of the permanent magnets is presented in Fig. 4, while the time variation of the average

number of particles per cluster is shown in Fig. 5. In this study, particles were considered to be in contact when the interparticle surface distance was less than 8% of the particle diameter. A group of contacting particles was defined as a single cluster, whereas isolated particles without any contact were not counted as clusters. The average number of particles per cluster was calculated as the total number of particles forming clusters divided by the number of clusters. Furthermore, Fig. 6 illustrates the time variation of the average velocity of particles after the initiation of the analysis.

From these results, it can be seen that in the early stage after the application of magnetization, both the number of clusters and the average number of particles increased with higher magnetization. This is because stronger magnetization enhanced the magnetic interactions between particles, leading to faster cluster formation. Consistently, the average particle velocity was also observed to increase with magnetization strength. Once the clusters stabilized, the number of clusters showed little change and eventually stabilized at a value independent of the magnetization strength.

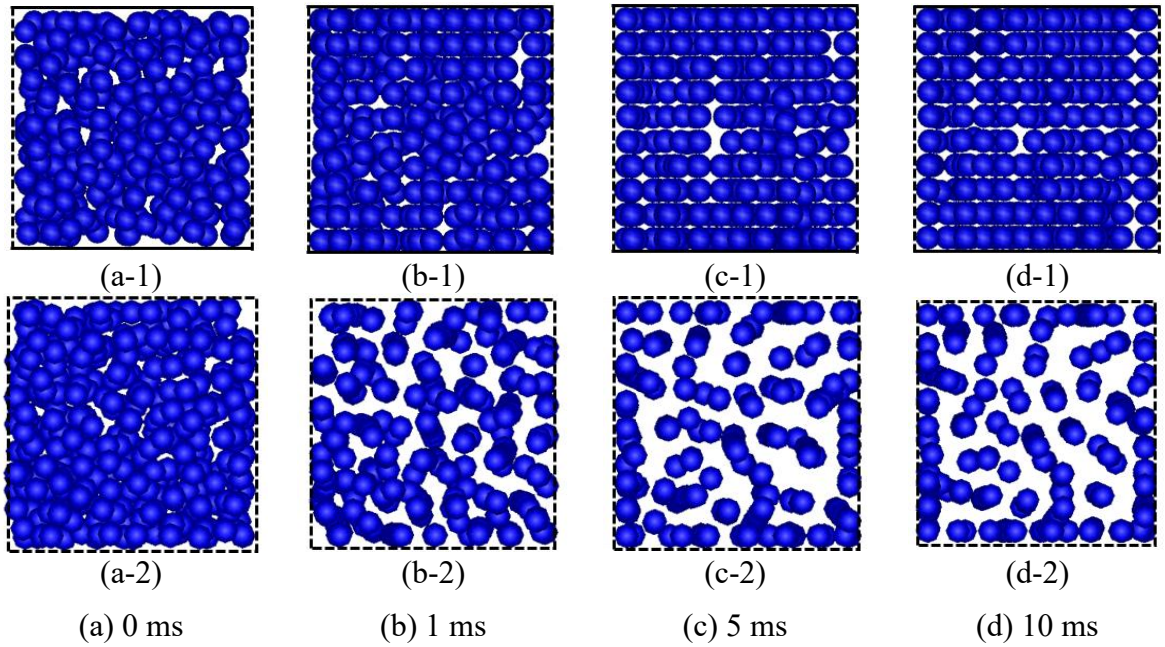

Fig. 3 Magnetic particles' behavior under magnetization of 0.3 T in stationary fluid. The snapshot is view from (1) -y-direction and (2) +z-direction.

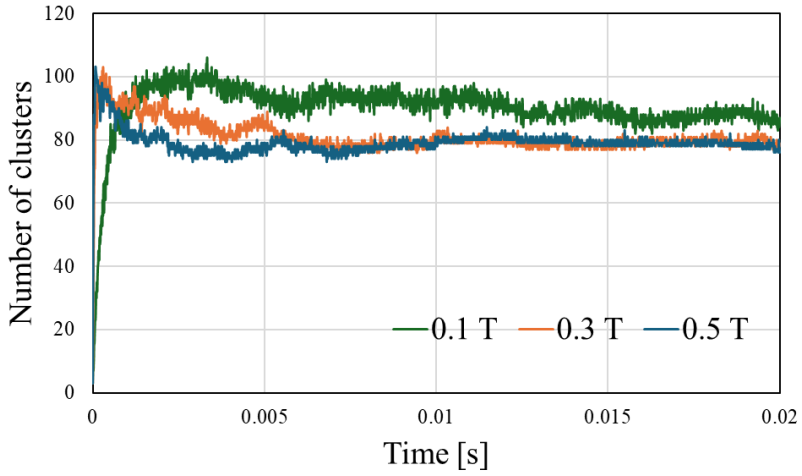

Fig. 4 Number of clusters in stationary fluid.

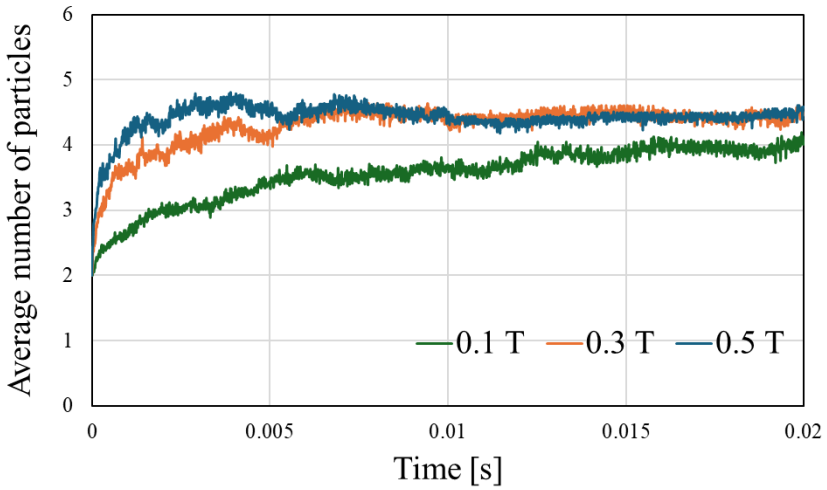

Fig. 5 Average number of magnetic particles per cluster in stationary fluid.

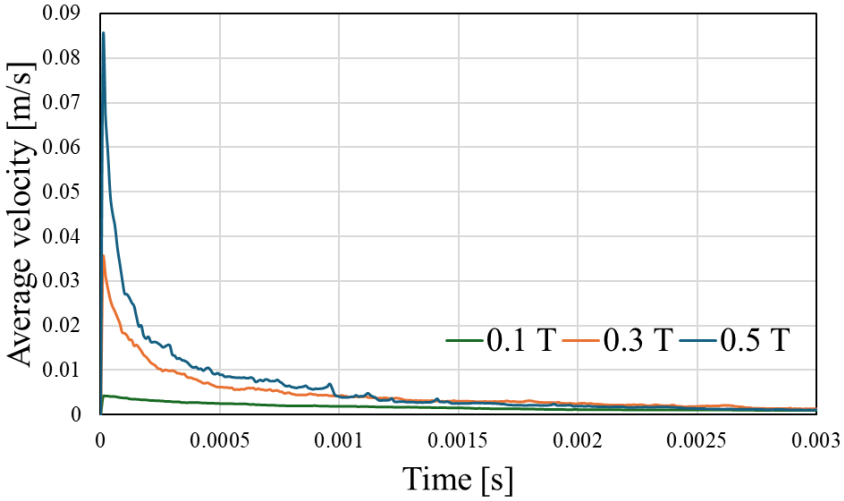

Fig. 6 Average velocity of magnetic particles in stationary fluid.

3.3 Magnetic particles behavior in shear flow

The case with shear flow under a magnetic field was next computed. In this setup, only the upper magnetic wall was translated in the positive x-direction at a constant velocity of 0.1 m/s from time $t = 0$, thereby imposing a shear rate.

The results of the analysis, for the case of magnetization of the permanent magnets at 0.3 T, are shown in Fig. 7. As in the stationary fluid, the particles were observed to form several chain-like clusters aligned with the magnetization direction. As time progressed, the system was influenced by the shear flow. As a result, the clusters tended to tilt toward the flow direction instead of aligning solely with the magnetization axis. This phenomenon can be attributed to particles colliding with the upper wall and receiving forces in the positive x-direction. The resulting motion is then transmitted sequentially to neighboring particles in contact, which leads to a change in the overall cluster orientation. Furthermore, the relative motion between particles arises from the competition between the interaction energy due to magnetization and the mechanical effects of shear. The balance between these factors determines both the stability of the clusters and their orientation.

The time variation in the number of clusters is shown in Fig. 8, and the time variation in the average number of particles per cluster is shown in Fig. 9. Both were found to be the same as in the stationary fluid during the initial stage of the analysis. However, even after the cluster structures stabilized, the number of clusters continued to fluctuate more than in the stationary fluid. This is considered to result from the repeated breaking and reformation of clusters due to the shear flow.

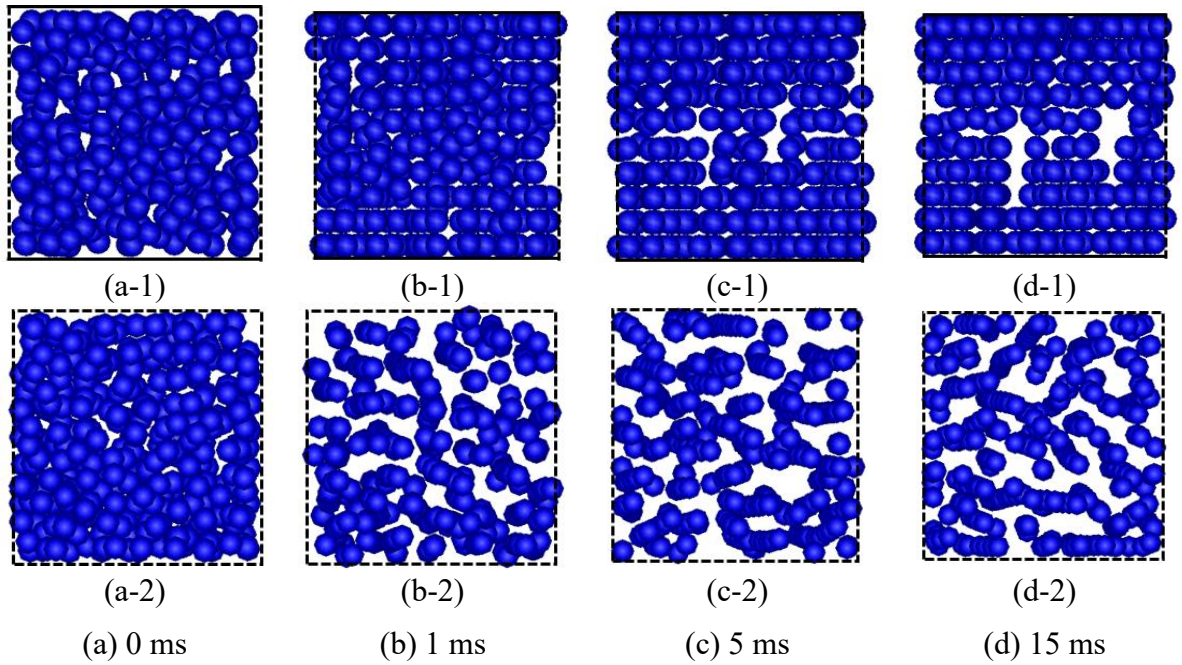

Fig. 7 Magnetic particles' behavior under magnetization of 0.3 T in shear flow. The snapshot is view from (1) -y-direction and (2) +z-direction.

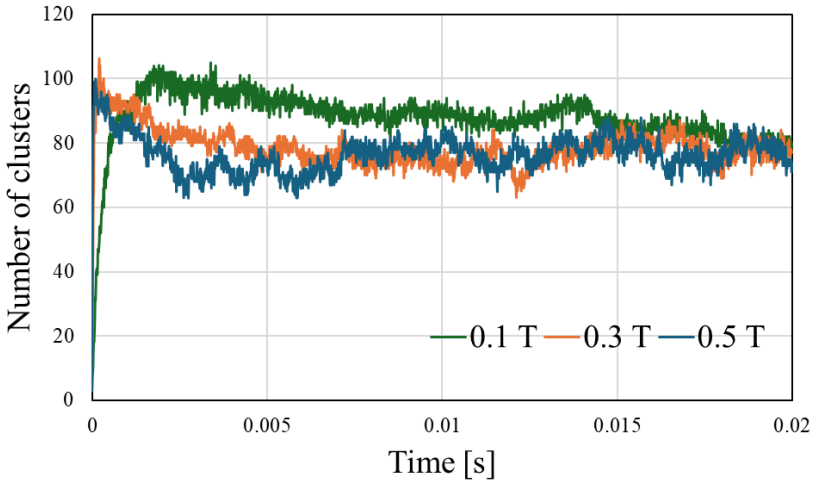

Fig. 8 Number of clusters in shear flow.

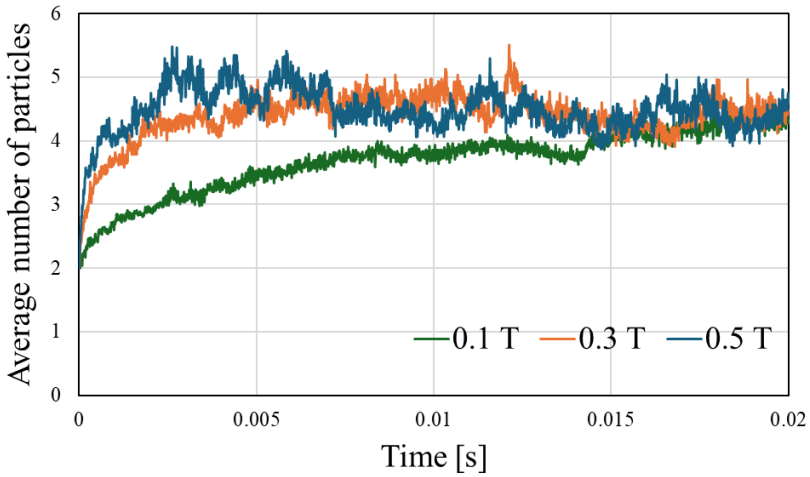

Fig. 9 Average number of magnetic particles per cluster in shear flow.

4 SUMMARY

This study proposed a numerical analysis method combining the particle method and the magnetic moment method to represent particle behavior in MR fluids. A simplified cubic model was used for the calculations. The results demonstrated the formation of clusters of magnetic particles aligned along the direction of the applied magnetic field. Also, The effect of the external magnetization strength on the cluster formation rate was also quantitatively evaluated. Furthermore, the tendency of clusters to incline in the flow direction under shear was confirmed. In future studies, the model will be extended to the full-scale MR damper intended for practical applications, and the analysis results will be compared with experimental measurements.

REFERENCES

[1] J. David Carlson and Mark R. Jolly, "MR fluid, foam and elastomer devices", Mechatronics, Vol. 10, pp. 555-569 (2000).

[2] A. Kimoto, "MR Damper Application Overview", Journal of the Robotics Society of Japan, Vol. 31, No. 5, pp. 483-485(2013).

[3] M. Mohebi and N. Jamasbi, "Simulation of the formation of nonequilibrium structures in magnetorheological fluids subject to an external magnetic field", Physical Review E, Vol. 54, No. 5, pp. 5407-5413(1996).

[4] Y. Ido, T. Inagaki, N. Umehara, "Numerical Simulations of Production Process of MAGIC Abrasive (Effect of Volume Fraction of Spherical Particles on Distribution of Particles)", Journal of JSAEM, Vol. 15, No. 3, pp. 341-347 (2007).

[5] T. Watanabe, M. Sakai, "Numerical Simulation of Magnetorheological Fluid with DEM-DNS Method", J. Soc. Powder Technol, Vol. 55, No. 8, pp. 426-432 (2018).

[6] T. Kawaguchi, T. Tanaka, Y. Tsuji, "Numerical Simulation of Fluidized Bed using the Discrete Element Method (the Case of Spouting Bed)", Trans. Japan Society of Mechanical Engineers Ser. B, pp. 79-85 (1992).

[7] O. Sano, "Forces on an Aerosol Particle in Low Reynolds Number Flow", Japan Association of Aerosol Science and Technology, Vol. 11, No. 4, pp. 290-294(1996).

[8] S. Matsuzawa, K. Mitsufuji, Y. Miyake, K. Hirata and F. Miyasaka, "Numerical Analysis of Electromagnetic Levitation Employing Meshless Method Based on Weighted Least Square Method", Journal for Manufacturing Science and Production, Vol. 15, No. 1, pp. 29-34 (2015).

[9] S. Matsuzawa, K. Mitsufuji, Y. Miyake, K. Hirata and F. Miyasaka, "Numerical Analysis of Electromagnetic Levitation Employing Meshless Method Based on Weighted Least Square Method", Journal for Manufacturing Science and Production, Vol. 15, No. 1, pp. 29-34(2015).